

Disruption of Synaptic Development and Ultrastructure by *Drosophila* NSF2 Alleles

BRYAN A. STEWART,* JOANNE PEARCE, MARTHA BAJEC,
AND RADHIKA KHORANA

Department of Life Sciences and Zoology, University of Toronto at Scarborough, Toronto,
Ontario M1C 1A4, Canada

ABSTRACT

First identified as the cytosolic component that restored intra-Golgi vesicle trafficking following N-ethylmaleimide poisoning, N-ethylmaleimide-sensitive factor (NSF) was later shown to be an ATPase that participates in many vesicular trafficking events. Current models hold that NSF disassembles postfusion SNARE protein complexes, allowing them to participate in further rounds of vesicle cycling. To further understand the role of NSF in neural function, we have embarked on genetic studies of *Drosophila* NSF2. In one approach, we employed transgenic flies that carry a dominant-negative form of NSF2 (*NSF^{E/Q}*). When expressed in neurons this construct suppresses synaptic transmission, increases activity-dependent fatigue of transmitter release, and reduces the functional size of the pool of vesicles available for release. Unexpectedly, it also induced pronounced overgrowth of the neuromuscular junction. The aim of the present study was twofold. First, we sought to determine if the neuromuscular junction (NMJ) overgrowth phenotype is present throughout development. Second, we examined *NSF2^{E/Q}* larval synapses by serial section electron microscopy in order to determine if there are ultrastructural correlates to the observed physiological and morphological phenotypes. We indeed found that the NMJ overgrowth phenotype is present at the embryonic neuromuscular synapse. Likewise, at the ultrastructural level, we found considerable alterations in the number and distribution of synapses and active zones, whereas the number of vesicles present was not changed. From these data we conclude that a primary phenotype of the *NSF2^{E/Q}* transgene is a developmental one and that alteration in the number and distribution of active zones contributes to the *NSF2^{E/Q}* physiological phenotype. *J. Comp. Neurol.* 488:101–111, 2005. © 2005 Wiley-Liss, Inc.

Indexing terms: neuromuscular junction; ATPase; vesicle; synapse

The quest for molecules that regulate vesicle trafficking led first to the isolation of N-ethylmaleimide-sensitive factor (NSF) because of its ability to restore vesicle transport in a Golgi transport assay (Block et al., 1988). This led to the further identification of soluble NSF attachment protein (SNAP) (Clary et al., 1990) and the SNAP receptors—Syntaxin, Vamp/Synaptobrevin, and SNAP-25—the SNARE proteins (Sollner et al., 1993). In the most current model of their function, the tripartite SNARE complex is thought to form the crucial elements required for membrane fusion, while the ATPase activity of NSF disassembles postfusion SNARE complexes, releasing the SNARE proteins to be re-used in further vesicle fusion events.

More recently, in addition to its canonical role in the SNARE cycle, other roles for NSF have been proposed (Whiteheart and Matveeva, 2004). The most widely stud-

ied non-SNARE role for NSF is in trafficking of postsynaptic AMPA-type glutamate receptors in the mammalian central nervous system (Nishimune et al., 1998; Osten et al., 1998; Song et al., 1998; Noel et al., 1999). This function may be a key regulator of synaptic strength. Additionally,

Grant sponsor: Natural Sciences and Engineering Research Council of Canada; Grant sponsor: Canada Foundation for Innovation; Grant sponsor: Canada Research Chairs Program.

*Correspondence to: Bryan A. Stewart, Dept. of Life Sciences, University of Toronto at Scarborough, 1265 Military Trail, Toronto, ON M1C 1A4, Canada. E-mail: stewart@utsc.utoronto.ca

Received 15 December 2004; Revised 16 February 2005; Accepted 19 February 2005

DOI 10.1002/cne.20603

Published online in Wiley InterScience (www.interscience.wiley.com).

the biochemical association of NSF with β -arrestin, GATE-16, Lma-1, and Rab6 (Morgan and Burgoyne, 1995; Xu et al., 1998; Han et al., 2000; Sagiv et al., 2000; Cong et al., 2001) indicate that NSF likely has an array of cellular functions, in addition to its role of disassembling the SNARE complex.

Unlike most species studied to date which have one isoform, *Drosophila melanogaster* has two NSF isoforms that share 80% amino acid identity (Boulianne and Trimble, 1995; Pallanck et al., 1995). Called NSF1 and NSF2, they can functionally substitute for each other (Golby et al., 2001) but NSF1 is the functionally predominant isoform in the adult central nervous system, while NSF2 is functional throughout development in neural and nonneural tissue. Null alleles of NSF1 die as pharate adults, while NSF2 null alleles die early as first instar larvae (Golby et al., 2001). Furthermore, there is no defect in synaptic physiology in *comatose* alleles of NSF1 at the larval stage (Mohtashami et al., 2001). In order to study synaptic development and function at the accessible third larval instar neuromuscular synapse, we generated dominant-negative NSF2 constructs (Stewart et al., 2001) that can be expressed in a tissue-specific manner. The design of the dominant-negative mutation was based on previous studies of mammalian NSF (Whiteheart et al., 1994) which showed that single amino acid substitutions within the ATPase domain of NSF severely reduces the ATPase activity of the molecule and single mutant subunits within the NSF oligomer substantially reduce the overall ATPase activity of NSF.

We previously showed that when the *Drosophila* dominant-negative NSF2 construct is expressed in neurons it suppresses synaptic transmission, reduces the size of the pool of releasable synaptic vesicles, and increases synaptic fatigue at the larval neuromuscular synapse (Stewart et al., 2002). Unexpectedly, we also observed a dramatic overgrowth of the neuromuscular junction. Such a phenotype is not predicted from the known biochemical function of NSF.

At present, several possible mechanisms may account for the overgrowth, one of which is that the altered morphology is a response to the concomitant alterations in neuromuscular physiology that occur in the *NSF2^{E/Q}* larvae. This seems unlikely, however, since mutants in the *n-synaptobrevin* and *syntaxin* genes that impair synaptic physiology to a level as severe as the *NSF2^{E/Q}* transgene do not have similar nerve overgrowth phenotypes (Stewart et al., 2000). Nevertheless, we reasoned that if such a mechanism were operating it would be less prominent early in synaptic development than at the third instar stage. Therefore, to address this possibility we asked whether the overgrowth phenotype can be detected early in development and if *NSF2* genetic loss of function alleles have a similar phenotype.

Second, one of the physiological defects in the *NSF2^{E/Q}* larvae is a reduced number of vesicles in the releasable pool (Stewart et al., 2002). Since NSF is known to be involved in many vesicle transport steps, this reduction in releasable vesicles may simply be due to fewer vesicles within the nerve terminal or it may be due to other structural or biochemical defects caused by *NSF2^{E/Q}*. While we previously showed that there are substantial numbers of vesicles at the *NSF2^{E/Q}* neuromuscular junction (Stewart et al., 2002), we did not quantitate the number of vesicles, or other ultrastructural features, in the previous report.

Further, the strength of synaptic transmission is often more strongly correlated with specific ultrastructural features of the nerve terminal (Cooper et al., 1995) than with features observable at the light microscopic level. For example, neuromuscular junctions that show morphological defects often maintain synaptic strength, if at the ultrastructural level the synaptic contacts and their active zones remain intact (Stewart et al., 1996). Therefore, in this study we also asked if there are ultrastructural correlates to the physiological and morphological *NSF2^{E/Q}* phenotypes previously observed.

Our results show that the overgrowth phenotype is present at the embryonic neuromuscular junction (NMJ) of both *NSF2^{E/Q}* and an *NSF2* loss of function allele and that there are substantial alterations in the synaptic ultrastructure of the *NSF2^{E/Q}* allele, including a reduction in the number of active zones per synaptic contact. Together, these data further our understanding of the consequences of *NSF2^{E/Q}* expression and suggest that the phenotypes associated with *NSF2^{E/Q}* are outside its established role in the SNARE cycle.

MATERIALS AND METHODS

Drosophila stocks

The *yw* strain was used as a control strain throughout. The UAS/GAL4 expression system was used to drive gene expression in the nervous system. To express transgenes specifically in nerve and not in muscle, the GAL4 driver line *elav-Gal4* was used. This line expresses GAL4 only in postmitotic neurons. *elav^{3A}-Gal4* is a P-element construct on the third chromosome comprising the *elav* promoter and *Gal4* coding sequence. Construction of the *UAS-NSF2^{E/Q}* line was previously described (Stewart et al., 2001). A recombinant third chromosome bearing *elav^{3A}-Gal4* and *UAS-NSF2^{E/Q}* was obtained by recombining the UAS transgene onto the same chromosome bearing *elav^{3A}-Gal4*. The recombinant chromosome was maintained in a *yw* background with the third chromosome balancer *TM3, Sb Ser y⁺*. For the electron microscopic studies herein we used *yw; elav^{3A}-Gal4: UAS-NSF2^{E/Q}/TM3 Sb,Ser,y+* larvae as our experimental subjects and the *elav^{3A}-Gal4* line and the *UAS-NSF2^{E/Q}* line as controls.

For the embryo studies undertaken here, virgin *yw* females was crossed to *yw; elav^{3A}-Gal4: UAS-NSF2^{E/Q}/TM3 Sb,Ser,y+* males. The resulting *yw; elav^{3A}-Gal4: UAS-NSF2^{E/Q}/+* embryos were identified by the reduced pigmentation of the denticle belts and mouth hooks in Stage 16 embryos. The *yw; +/TM3 Sb,Ser,y+* siblings served as controls.

The genetic loss of function allele *NSF2⁵⁵* was generously supplied by L. Pallanck (Univ. of Washington) and is described in Golby et al. (2000). These alleles were maintained with *TM3, KrGFP* balancers and homozygous mutant embryos were identified by lack of GFP signal. *NSF2⁵⁵/TM3 KrGFP* siblings served as controls.

Embryo collection and dissection

For analysis of embryonic NMJs, adult flies of the appropriate genotype were allowed to lay eggs on grape-agar medium. Typically, the adults were kept on medium for 4–6 hours in the afternoon, the medium removed, and the embryos were allowed to develop overnight at room temperature (22–23°C). Embryos were then dechorionated by

hand on double-sided tape and Stage 17 embryos were selected for dissection. These embryos were removed from the vitelline membrane under HL3 saline (Stewart et al., 1994) using glass or tungsten dissecting needles. Their heads and tails were then glued to the Sylgard-coated slides, using Nexaband glue, and a dorsal midline incision was made using the needles. The digestive system and fat tissue were removed and the cuticle laid out along the incision and glued to the slide.

Immunofluorescence, image acquisition, and analysis

Following dissection, the preparations were immediately fixed in 3.7% formaldehyde in phosphate-buffered saline (PBS), pH 7.2, for 10–20 minutes. They were then washed on the slide for 3×5 minutes in PBT (PBS plus 0.1% Triton X-100) and stained with FITC-conjugated goat anti-HRP, an antibody that labels *Drosophila* neurons, for 1 hour at room temperature. Following antibody labeling the preparations were washed in PBT, mounted in Vectashield, and coverslipped.

Images were acquired on a Zeiss LSM510 confocal microscope using the 488 line of an argon laser with a 530 nm long-pass filter. A $63\times$, 1.3 n.a. oil immersion lens was used to acquire Z-sections that were acquired with the pinhole aperture set to acquire images of 1 μm thick. Image sections were then projected onto a single plane and nerve terminal branch lengths were measured using ImageJ software.

Electron microscopy

To process the tissue for ultrastructural analysis, we followed the method of Atwood et al. (1993). Wandering third instar larvae were dissected in HL3 physiological solution and fixed in 0.1 M sodium cacodylate buffer (pH 7.4) containing 1% glutaraldehyde and 4% formaldehyde for 2 hours at room temperature. Following 15 minutes of rinsing in 0.1 M sodium cacodylate, the tissue was post-fixed for 30 minutes in 1% osmium tetroxide in 0.1 M sodium cacodylate. The tissue was then dehydrated through an ethanol series and individual abdominal hemisegments 3 or 4 were dissected from the larvae and embedded in Epon-Araldite resin.

The resin blocks were trimmed and thick cross-sections were taken to identify the bodywall muscles. Upon identification of an area of innervation, thin sections (75–100 μm) were cut and collected on Formvar-coated slot grids and doubly stained with uranyl acetate and lead citrate, then examined with a Hitachi H-7500 electron microscope. Images were either collected digitally on a MegaView II camera or by taking photomicrographs.

The ultrastructural data from mutant larvae in this report is based on two separate serials totaling 194 sections from one *yw; elav^{3A}-Gal4: UAS-NSF2^{E/Q}/TM3 Sb, Ser,y+* larvae. We additionally collected a third series of sections from a second mutant larvae that consisted of 370 sections ($\sim 27 \mu\text{m}$), that were periodically examined; that examination confirmed our results from the more detailed measurements. For controls, the serial sectioning consisted of one series containing 102 sections from a *elav^{3A}-Gal4* larva. In total, we measured data from 11.7 μm of nerve terminal from the control and 24.5 μm of nerve terminal from the *NSF2^{E/Q}* strain.

Data analysis

Data were compiled and analyzed in Prism3 software (GraphPad, San Diego, CA). Student's *t*-test was used to test for statistically significant differences between two genotypes, while one-way ANOVA was used for multiple genotype comparisons, with Dunnett's multiple comparison test used for post-hoc analysis of the difference between experimental and control genotypes.

RESULTS

Early developmental defects at NSF2 mutant NMJs

A previous report on the effects of neural expression of dominant-negative NSF2 in *Drosophila* neurons showed that there is dramatic overgrowth of the neuromuscular junction in third instar larvae; the total branch length in such larvae is nearly double that of control larvae (Stewart et al., 2002). Examples of larval neuromuscular junctions from three control strains and the *NSF2^{E/Q}* strain are shown in Figure 1. In order to distinguish between the possibilities that the overgrowth phenotype is present early in development or acquired later, we examined NMJ morphology at the embryonic NMJ and found that the NMJ show signs of overgrowth and hypersprouting at this early developmental time point (Fig. 2). To quantify the overgrowth we measured the total branch length on muscle 6 and 7 in abdominal segments 3 and 4 for each of the control and *NSF2^{E/Q}* strains. In control embryos the total branch length was $29.2 \pm 1.3 \mu\text{m}$ ($n = 13$) whereas *NSF2^{E/Q}* neuromuscular junctions were $42.8 \pm 2.0 \mu\text{m}$ ($n = 18$). We additionally analyzed a homozygous NSF2 loss of function mutation, *dNSF2⁵⁵*, in this manner. We found that the total branch length in these mutants was $37.6 \pm 3.5 \mu\text{m}$ ($n = 9$) in length. Each of the differences between each of the mutants and the control lines was significantly different (ANOVA, $P < 0.05$). These data therefore show that NMJ overgrowth is present early in development and that the *NSF2^{E/Q}* transgene phenocopies a *NSF2* loss of function mutation.

Synaptic ultrastructure of *NSF2^{E/Q}* larvae

Stewart et al. (2002) previously reported the effects of expressing dominant-negative NSF2 on the morphology and physiology of the third instar NMJ. Among the findings, in addition to the hypersprouting phenotype noted above, was the observation that there is a substantial impairment of synaptic physiology including a reduction in the number of releasable synaptic vesicles. While they provided evidence that there were abundant small clear vesicles at the mutant nerve terminal, a careful examination of synaptic ultrastructure was not performed at that time. Here we present a more detailed analysis of the nerve terminal ultrastructure derived from serial section electron microscopy.

To accurately quantitate the nerve terminal ultrastructure we collected series of contiguous ultrathin sections in order to reconstruct those areas of the nerve terminal. Table 1 summarizes the nerve terminal, synaptic, and active zones measurements we made. Two motor nerve terminals, called Ib and Is, innervate abdominal muscles 6 and 7 and like previously published reports (Atwood et al., 1993; Stewart et al., 1996) we identified these terminals on the basis of mitochondrial

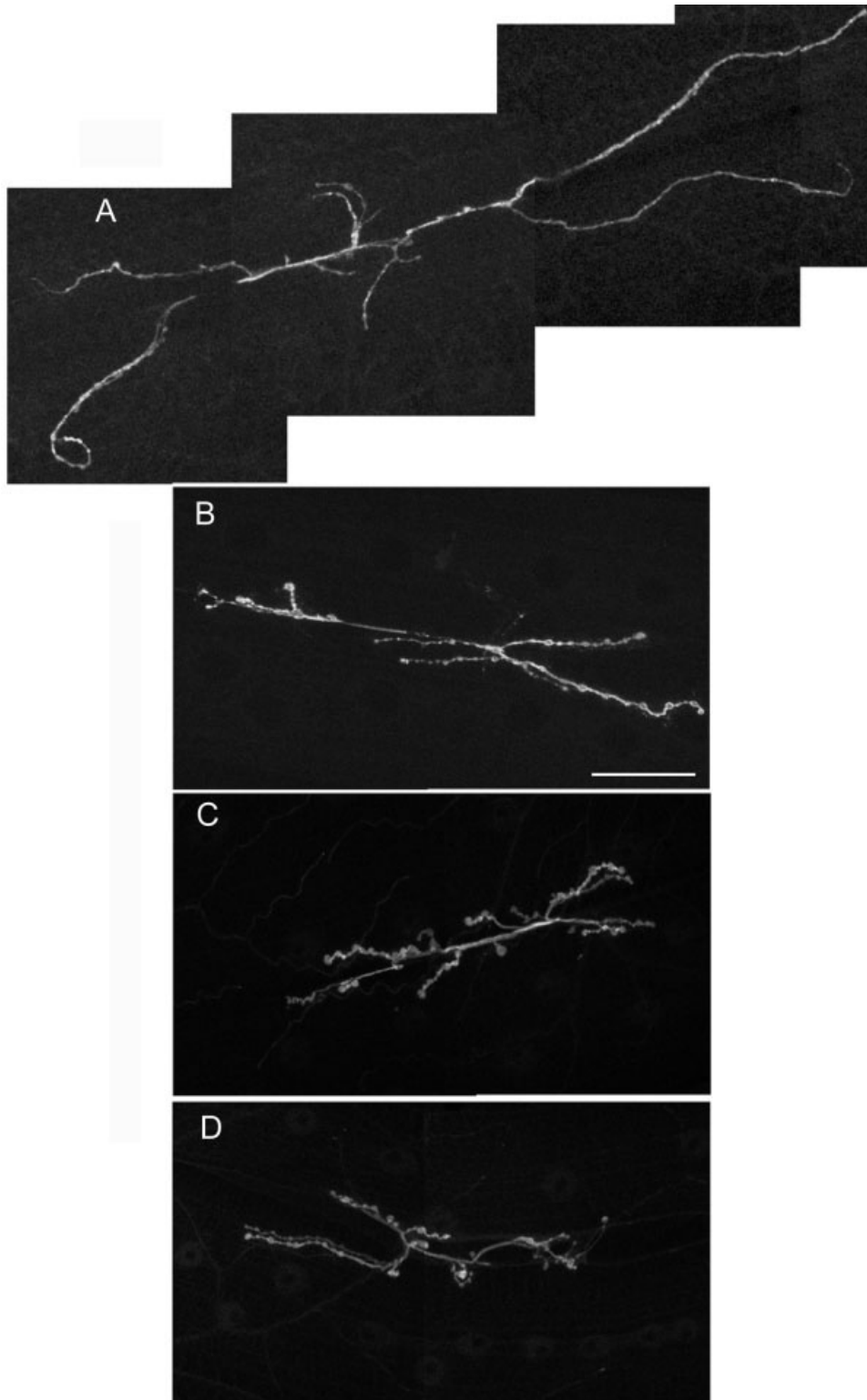


Fig. 1. *NSF2^{E/Q}* induces nerve terminal overgrowth. Representative neuromuscular junctions (NMJs) from third instar *Drosophila* larvae. **A:** *yw; elav^{3a}-Gal4: UAS-NSF2^{E/Q}/+*. **B:** *yw* control strain. **C:** *UAS-EC2*. **D:** *elav^{3a}-Gal4*. All of the images were acquired at the same magnification. A: A montage of four 512×512 pixel images was required to capture the entire NMJ in A, whereas only two 512×512 pixel images were required for the control strains in panels B–D. Scale bar = $50 \mu\text{m}$ in B (applies to A–D).

abundance, the relative abundance of dense core vesicles, and the extent of the underlying muscle sarcoplasmic reticulum and collected separate data for each of them. Figure 3 shows sample electron micrographs of

the mutant and control NMJs in which two axon profiles are visible in each image. Also labeled on these images are synaptic contacts, synaptic vesicles, and, in the control sample, an active zone T-bar.

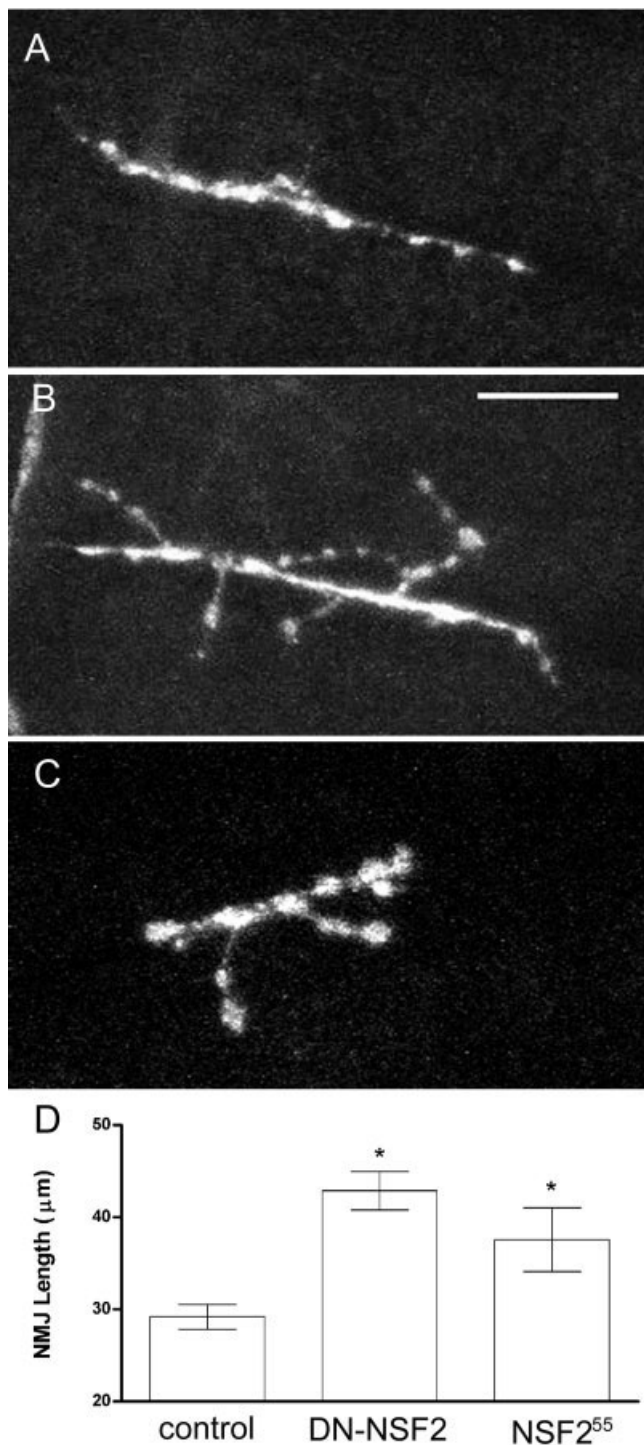


Fig. 2. Early synaptic defects in *NSF2* alleles. Representative fluorescent images of embryonic neuromuscular junctions in (A) *yw: +/TM3, Sb, Ser, y+* controls; (B) *yw; elav^{3A}-Gal4: UAS-NSF2^{E/Q}/+*; and (C) *NSF2⁵⁵/NSF2⁵⁵* alleles. D: Quantitation of total NMJ length from the indicated genotypes. Sample size: $n = 13$ controls, $n = 18$ *NSF2^{E/Q}*, and $n = 9$ *NSF2⁵⁵*. Bars represent mean \pm SEM. Asterisks indicate significant differences at $P < 0.05$. Scale bar = $10 \mu\text{m}$ in A–C).

Qualitatively, the mutant nerve terminals are characterized by thinner processes and long stretches of nerve terminal devoid of synaptic contacts. We did not take serial section data from such regions, but rather from areas with recognizable synaptic contacts. The data in our table thus likely represent a best-case report of the ultrastructural features in these neurons.

Upon examining and reconstructing the serial section images, we first identified and measured the synaptic contacts and found that there were fewer synapses for a defined nerve terminal length (Table 1). This was also evident from a third serial section that we did not quantitate. The mean size of the synapses, however, was not different, with values near $0.4\text{--}0.5 \mu\text{m}^2$ for each of the nerve terminal types in each genotype. Thus, one ultrastructural correlation of the *NSF2^{E/Q}* phenotype is a spatial redistribution of synapses along the length of the nerve terminal without an effect on individual synapse size.

Synaptic vesicle release is thought to occur at synaptic active zones. At the ultrastructural level active zones in *Drosophila* are thought to correspond to densely staining T-bar structures associated with synaptic contacts. We therefore examined the occurrence of active zones in *NSF2^{E/Q}* and control samples and found substantial differences between the genotypes. By counting the number of active zones on each synapse we found that, on average, there are about half as many active zones per synapse in the *NSF2^{E/Q}* synapses compared to the control (Table 1). This is a statistically significant difference (t -test; $P < 0.05$). Since the individual synapses size is not different between the genotypes, there is a resulting reduction in the number of active zones for each μm^2 synaptic contact. For example, we observed about four active zones for each $1 \mu\text{m}^2$ of synaptic contact in the controls but only two active zones per μm^2 in the *NSF2^{E/Q}* synapses.

In many systems there is a correlation between the active zone density and synaptic strength; we therefore examined the frequency distribution of the number of active zones on each synapse. For the controls, many synapses had at least one active zone and a substantial proportion of synapses had more than one active zone; only 10% of Ib synapses and 20% of Is synapses had no active zones in the control. Examples of control boutons showing multiple T-bars on each synapse are shown in Figure 4. The images represent five adjoining sections through the nerve terminal with several T-bars appearing through the sequence. In our estimation, the T-bar marked with the arrowhead appears in the first section, then there are two intervening sections, and then a second T-bar appears marked with a double asterisk. In contrast, the mutant synapses had much higher proportions with 0 or 1 active zone, a small fraction had 2 active zones, and no synapses had >2 active zones. Where we did see T-bars in the mutants they appeared normal; a detail of one is shown in Figure 5. Altogether, these data show that despite the synapses in the two genotypes being of similar size, the number active zones per synapse is greatly reduced in the mutant.

Lastly, we examined the number and distribution of synaptic vesicles near active zones in the nerve terminals from randomly selected sections. In both of the genotypes there were accumulations of synaptic vesicles near synaptic contacts. We examined the number of vesicles within 50 nm of the plasma membrane, the number associated

TABLE 1. Ultrastructural Data from Serial Section Electron Microscopy of Control and *NSF2^{E/Q}* Nerve Terminal

Bouton type	Control		<i>NSF2^{E/Q}</i>	
	Is	Ib	Is	Ib
Length examined (μm)	5.8	5.9	9.1	15.4
Number of synapses examined	15	20	14	23
Total synaptic area (μm^2)	5.7	10.3	6.3	10.5
Mean synaptic area (μm^2)	0.38 ± 0.14	0.52 ± 0.08	0.45 ± 0.06	0.46 ± 0.05
Synaptic area/ μm terminal	0.98	1.8	0.69	0.68
Number AZ observed	26	41	11	19
Number AZ/synapse	1.7 ± 0.58	2.1 ± 0.30	0.79 ± 0.15	0.79 ± 0.14
Number AZ/ μm terminal	4.5	7.0	1.2	1.2
Number AZ/synaptic area (μm^2)	4.5	3.9	1.8	1.8
Total AZ length (μm)	3.8	6.5	1.9	2.9
Mean AZ length (μm)	0.14	0.16	0.17	0.15
% of synapses with:				
0 active zones	20	10	29	22
1 active zone	47	30	64	63
2 active zones	20	25	7	15
>2 active zones	12	35	0	0
Vesicle data				
Number w/in 150 nm arc of AZ	23.1 ± 1.2	26.6 ± 1.6	33.4 ± 6.8	41.5 ± 4.1
Number membrane-bound	6.1 ± 0.72	7.0 ± 0.61	8.4 ± 1.9	9.4 ± 1.0
Number dense bar-bound	10.6 ± 1.0	11.1 ± 0.71	11.2 ± 1.8	14.8 ± 1.8

AZ, active zone.

with the active zone T-bar, and the number within a 150-nm arc about the active zone T-bar. None of these measures showed significant differences between the genotypes except for the number of vesicles within the 150-nm arc of the type Ib boutons.

To address whether there is a reduction in the number of synaptic vesicles in the mutant larvae, we counted the total number of vesicles in cross-sections of the nerve terminals. We found on average that there were 225 ± 20 ($n = 13$ cross sections) vesicles in the mutant and 164 ± 25 ($n = 14$ cross sections) vesicles in the controls. This difference was not significant. Likewise, when we analyzed a different set of cross sections and normalized for the cross-sectional area of the profile, there were no significant differences. The control showed 201 ± 38 vesicles/ μm^2 , while the *NSF2^{E/Q}* showed 150 ± 30 vesicles/ μm^2 ($n = 7$ profiles each). Thus, there were no detectable differences in the abundance of synaptic vesicles within the nerve terminals that we examined. Therefore, the major ultrastructural effects that we detected in the *NSF2^{E/Q}* larvae were a reduction in the number of synapses along the nerve terminal and reduction in the number of active zones found on each synapse.

DISCUSSION

In order to examine the role of NSF, we have been studying the effects of a dominant-negative NSF2 transgene expressed in *Drosophila* neurons. The use of this transgene allows us to perturb NSF function while preserving the viability of the animals such that we can examine the well-characterized third larval instar NMJ; loss of function alleles of NSF2 are lethal at the first instar stage (Golby et al., 2001). The present study focused on two previously unresolved issues: first, does the *NSF2^{E/Q}* phenotype appear early in development or is it a later response to impaired synaptic physiology; and, second, are there ultrastructural changes that correlate to the previously reported changes in synaptic morphology and function. The results unequivocally show that the *NSF2^{E/Q}* phenotype does appear early in development, that this phenocopies an *NSF2⁵⁵* loss of function allele, and that

there are substantial alterations in synaptic ultrastructure of the *NSF2^{E/Q}* nerve terminal.

Early developmental phenotype

In *Drosophila*, neuromuscular synaptogenesis begins about 13–15 hours after egg laying at 25°C (Broadie and Bate, 1993) and the embryos we examined here were about 17–19 hours old. Our results undeniably show that the *NSF2^{E/Q}* phenotype is present very early in the life of the synapse, and indeed a similar phenotype is present in the *NSF2⁵⁵* loss of function allele. The latter point is important since it supports the fact that *NSF2^{E/Q}* represents a bona fide *NSF2* phenotype. A previous investigation of *NSF2* loss of function alleles did not examine embryonic NMJ morphology, so this is the first report of such a phenotype (Golby et al., 2001). It is also worthwhile noting that downregulation of NSF in mammalian hippocampal neurons leads to neurite outgrowth (Yu et al., 2002), signifying that the overgrowth phenotype is not specific to *Drosophila* but is likely to be a common feature of NSF activity. Interestingly, overexpression of NSF's binding partner α -SNAP in the *Drosophila* wildtype background produces a phenotype opposite to the *NSF2^{E/Q}* phenotype: namely, reduced nerve terminal branches (Babcock et al., 2004). It remains to be determined if α -SNAP loss of function mutants display an NMJ morphological phenotype, but the overexpression result indicates both NSF and α -SNAP may play a role. Additionally, we recently demonstrated (Laviolette et al., 2005) that expression of a *UAS-Snap* transgene can restore the *NSF2^{E/Q}* neuromuscular overgrowth phenotype. Altogether, these data clearly establish a role for NSF/ α -SNAP in synaptic development.

Previous examination of *NSF2^{E/Q}* showed a dramatic overgrowth of the NMJ in the third larval instar in addition to impaired synaptic physiology (Stewart et al., 2002). The overgrowth phenotype was a surprising one and several potential explanations for it remain open. One possible explanation is that the nerve terminal expands in response to the functional impairment. We think that explanation is unlikely because hypomorphic alleles of the SNARE proteins *n-synaptobrevin* and *syntaxin*, which re-

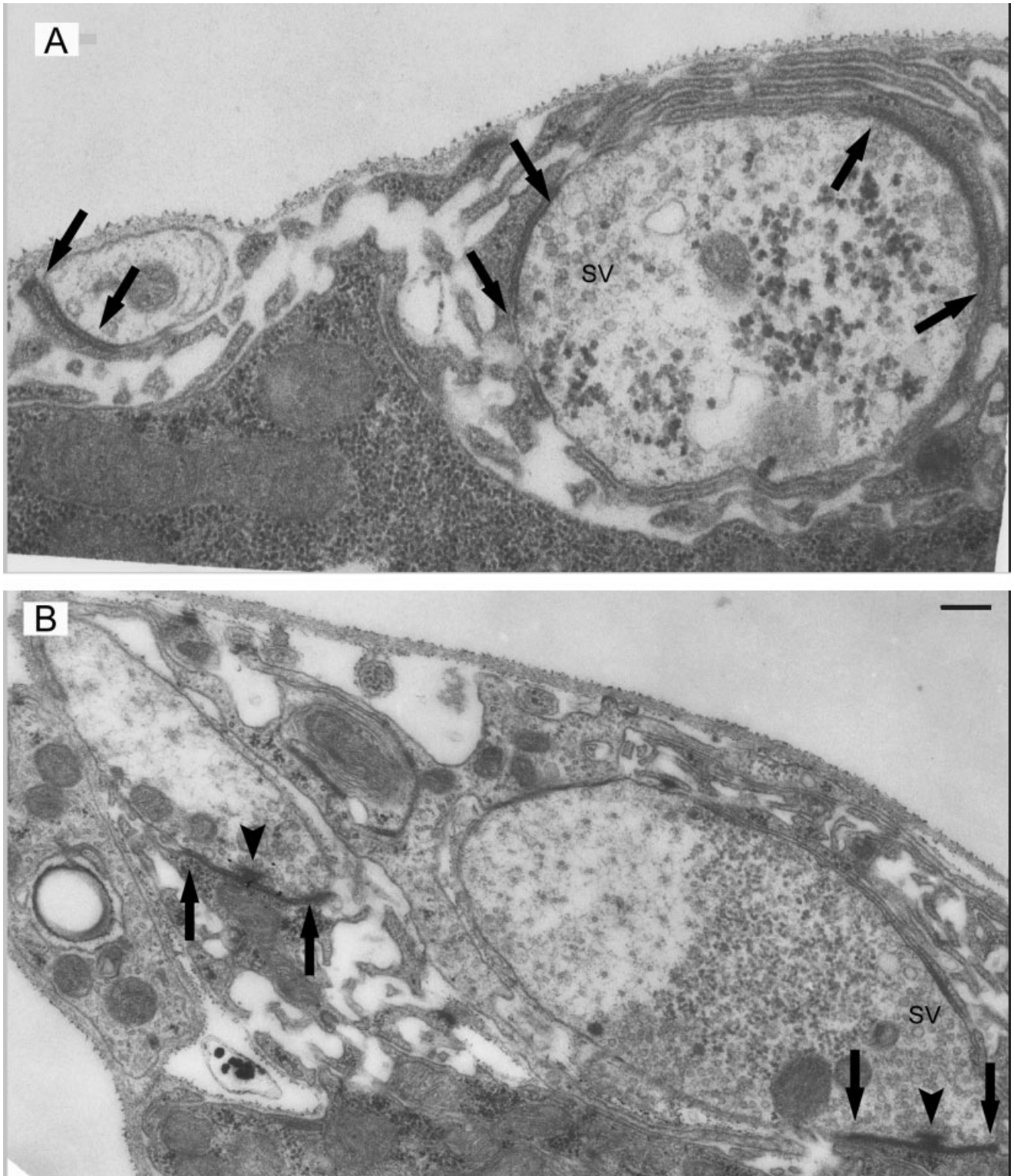


Fig. 3. Nerve terminal ultrastructure. The upper and lower images represent electron micrographs obtained from *NSF2^{E/Q}* and control larvae, respectively. Noted on the images are synaptic vesicles (SV), synaptic contacts (arrows), and active zone T-bars (arrowhead). Scale bar = 300 nm in A (applies to A,B).

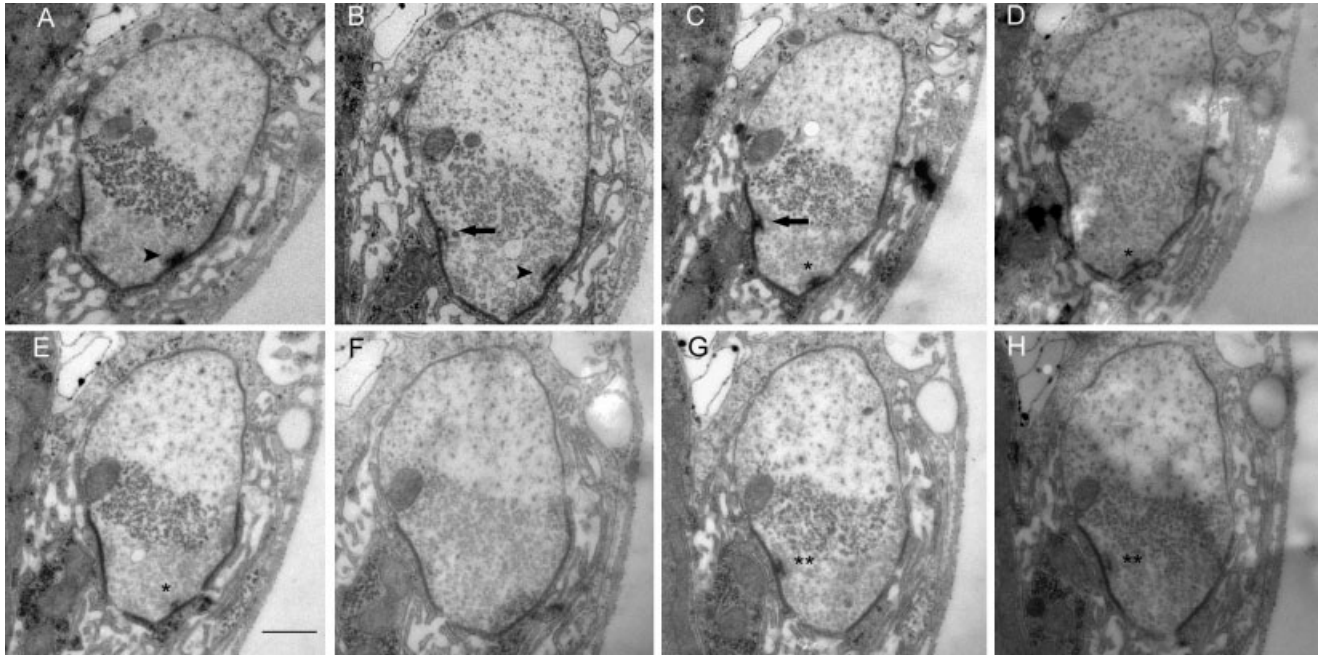


Fig. 4. Multiple active zones per synaptic contact. This series of eight images illustrates multiple T-bars found on individual synaptic contacts in the control animals. In (A) one T-bar is marked by an arrowhead; in (B) a second T-bar, marked by the arrow appears on a neighboring contact; in (C) a third T-bar marked by an asterisk

appears, while the one marked by the arrowhead is gone; in (D,E) only the T-bar marked by the asterisk is present; in (F) there are none visible. In (G,H) a fourth T-bar has appeared on the same synaptic contact as in B and C. Scale bar = 500 nm in E (applies to A–H).

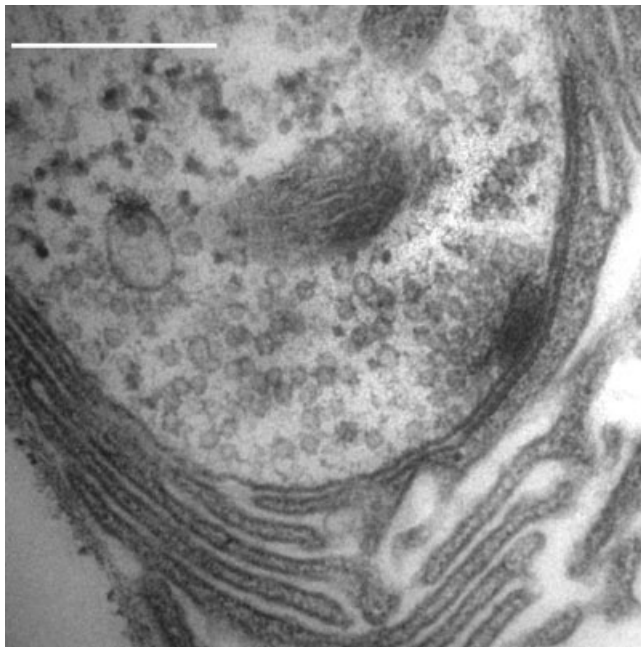


Fig. 5. T-bar in *NSF2^{E/Q}* larvae. While there were not many T-bars in the *NSF2^{E/Q}* sample, were they did occur they appeared as they do in the control samples. This images shows the platform-shaped structure and aggregation of vesicles around the T-bar from an *NSF2^{E/Q}* synapse. Scale bar = 500 nm.

duce synaptic transmission to levels seen in *NSF2^{E/Q}*, do not have a comparable morphological phenotype (Stewart et al., 2000). Likewise, severe alleles of *synaptotagmin* substantially reduce synaptic output without inducing nerve terminal overgrowth (DiAntonio and Schwarz, 1994). Therefore, a reduction in synaptic strength by itself does not appear to be causative factor controlling nerve terminal expansion.

Our data clearly show that nerve terminal overgrowth occurs very early in development of the *NSF2^{E/Q}* nerve terminal. It is difficult to rule out the possibility of feedback from the muscle to the nerve as a factor in this phenotype because we simply do not know the period of time such a mechanism would require. However, we observe nerve terminal expansion within a few hours of synaptogenesis in *NSF2^{E/Q}* embryos and we think it is unlikely that such retrograde signaling and remodeling could occur in the short period of time between synaptogenesis and when we examine the embryonic NMJ. We therefore favor the idea that the overgrowth phenotype is primarily an autonomous developmental phenotype and that it is not secondary to changes in synaptic physiology.

Nerve terminal ultrastructure

Our results on the changes in nerve terminal ultrastructure help us to more fully understand the effects of *NSF2^{E/Q}* expression and delineate the underlying causes of the physiological and developmental phenotypes.

One of the major differences observed in the mutant was a reduction by one-half of the number of synaptic contacts per μm of nerve terminal length. However, considering that the total length of all the nerve terminal branches is

about doubled in the mutant strain (Stewart et al., 2002), there appears to be conservation of the total number of synaptic contacts throughout the entire NMJ in the control and mutant strains. Therefore, rather than the absolute number of synaptic contacts being the key factor, the spatial distribution of the synapses may be more important to the *NSF2^{E/Q}* physiological phenotype.

The second major difference was in the number of active zones found on the individual synapses. In this case there appears not to be a conservation in the total number across the genotypes, since the number of active zones per μm of terminal length in the mutant is about one-fourth that found in the control, whereas the total length is about doubled. Thus, to a first approximation there would be one-half the total number of active zones in the mutant larval NMJ. Since the active zones are believed to be a site of vesicle release, the decrease in the number of active zones would strongly indicate that a major factor underlying reduced synaptic strength in the *NSF2^{E/Q}* larvae is a reduction in release sites.

It is also important to note that not only is the number of active zones reduced, but their distribution upon synapses is also different. Many of the control synapses have more than one active zone per contact but these are rare in the *NSF2^{E/Q}* mutant, with many synapses having only one active zone and a sizable fraction having none. Our previous physiological study showed a nearly 5-fold reduction in synaptic output at external calcium concentrations of 1.0 and 1.5 mM, values in the physiological range (Stewart et al., 2002). While the total number of active zones is reduced, they are reduced by one-half and this may not fully account for the physiological impairment. However, if we examine the synapses in which there are two or more active zones we find that there is a 5-fold reduction in the Is terminal and a 4-fold reduction in the Ib terminal. Therefore, a strong correlation can be made between impaired synaptic output and the reduced number of synapses with two or more active zones. This observation is in accord with previous studies on crustacean synapses that showed a strong correlation between the number of active zones on each synapse and synaptic strength (Cooper et al., 1995, 1996). If presynaptic calcium channels are associated with the active zones, then this correlation might arise from the intermixing of calcium from multiple sources to effectively increase the intracellular calcium concentration (Llinas et al., 1992; Cooper et al., 1996). The present results follow the same pattern in that the nerve terminal with fewer active zones per synapse is weaker than the nerve terminal with more active zones per synapse.

Finally, our previous study (Stewart et al., 2002) showed that in neurons expressing *NSF2^{E/Q}* there are fewer synaptic vesicles in the releasable pool. While we showed that there were abundant vesicles in the nerve terminal, here we further demonstrate that there is no significant reduction of vesicle number in the mutant, and therefore we think that a major change in vesicle population is an unlikely explanation for the 80% reduction in the size of the releasable pool of vesicles. It may appear that our sampling biases us towards this conclusion since we have taken these data from synaptic areas, while a confounding feature of the *NSF2^{E/Q}* ultrastructure is fewer synapses per length of nerve terminal. However, since vesicle clusters are associated with synaptic areas and there appears to be an overall conservation of synapse

number between the mutant and controls, we likewise think that there is an overall conservation of vesicle number. Therefore, the reduced size of the releasable vesicle pool does not appear to be simply related to an overall reduction in vesicle number. Rather, the inability of the vesicles to enter the releasable pool may be due to an altered biochemical state of the vesicles. We previously found no change in the abundance of SNARE complexes in the *NSF2^{E/Q}* adult or larval brain (Stewart et al., 2002), suggesting that either another of NSF's biochemical partners is required for this task or, alternatively, that the vesicles have reduced ability to move within the nerve terminal boutons.

In developmental contexts, NSF-dependent trafficking has been studied at the developing *Drosophila* wing margin (Stewart et al., 2001), but NSF has not been previously assigned a role in synaptic development. In some cases SNARE proteins have been associated with developmental function and, by association, NSF may be implicated (Hepp and Langley, 2001; Kimura et al., 2003). However, the overall role of SNARE-mediated transport in the developing growth cone and in synapse formation is not clear; in some systems SNARE-dependent vesicle transport seems to be an important component of growth cone function but in others it is not so. In particular, SNAP-25 (Osen-Sand et al., 1993) and a tetanus toxin-insensitive form of VAMP (Martinez-Arca et al., 2000) have been shown to contribute to neurite extension in experiments using cortical and amacrine neural cell cultures and PC12 cell assays. However, genetic deletion of *syntaxin*, *n-synaptobrevin*, or *SNAP-25* does not apparently affect *in vivo* neural synapse development in *Drosophila* (Schulze et al., 1995; Deitcher et al., 1998; Vilinsky et al., 2002). Identification of developmental defects associated with NSF may point to new roles for this molecule and help to resolve the role of SNAREs in synapse formation.

How could modulation of NSF lead to the results we found? Recent genetic studies of *NSF2^{E/Q}* from our laboratory (Laviolette et al., 2005) provide a framework for understanding the novel phenotypes reported here. In a screen to identify genes that interact with the *NSF2^{E/Q}* overgrowth phenotype we found that upregulation of several groups of genes can suppress the *NSF2^{E/Q}* phenotype (Laviolette et al., 2005). Importantly, upregulating components of the actin cytoskeleton potently suppress the phenotype. Three lines of evidence lead us to speculate that disruption of actin biochemistry is the underlying cause of the *NSF2^{E/Q}* phenotype. First, there is likely a vesicular trafficking role for actin within the presynaptic nerve terminal, although the precise function remains controversial (Doussau and Augustine, 2000). While there is evidence that actin is an important component of the endocytic pathway (Shupliakov et al., 2002), its role in the exocytic pathway is unclear. Some studies report a restraining role for actin (Morales et al., 2000), some reporting a supportive role (Sankaranarayanan et al., 2003), and others support a positive function (Cole et al., 2000; Zhang and Benson, 2001; Sakaba and Neher, 2003). In any case, since some of the vesicles at the *NSF2^{E/Q}* nerve terminals seem not to be able to be released, a defect in intra-bouton mobility is possible. Second, actin is well known to be important for growth cone movement, and regulation of actin is essential to synaptogenesis (Zhang and Benson, 2001). Misregulation of actin might explain the early nerve overgrowth phenotype we see. Third, we have pre-

viously shown that there is a considerable fraction of *Drosophila* NSF1 normally found in noncytosolic cell fractions (Mohtashami et al., 2001) and (Phillips et al., 2001) have demonstrated that actin and NSF are components of the presynaptic particle isolated from rat synaptosomes. To the extent that the mammalian presynaptic particle is equivalent to the *Drosophila* T-bar active zone, it is reasonable to think that disruption of NSF activity may lead to perturbation of presynaptic particle integrity and the alterations in active zone number we report here. Thus, the disparate phenotypes we observe with respect to physiology, morphology, and ultrastructure in the *Drosophila* *NSF2^{E/Q}* allele may have a common root in perturbation of the actin cytoskeleton. Our future studies will be aimed at testing this hypothesis. Interestingly, it was recently shown that mutation of the *Drosophila* gene *nervous wreck* (*nwk*) causes phenotypes remarkably similar to the *NSF2^{E/Q}* phenotype (Coyle et al., 2004). *nwk* is an SH3 adaptor protein that interacts with WASP, a well-known regulator of actin dynamics.

In summary, here we present evidence to show that the *NSF2^{E/Q}* mutant phenotype is present early in neuromuscular development, that it phenocopies an *NSF2* loss of function allele, and is associated with substantial ultrastructural rearrangements. These data lead us to the conclusion that the defects associated with *NSF2^{E/Q}* are developmental. Future studies that investigate the relationship between the developmental and physiological defects of *NSF2^{E/Q}*, and whether they are separable, will prove invaluable to our understanding of the relationship between synapse structure and function.

ACKNOWLEDGMENT

BAS is a member of the CFI Centre for the Neurobiology of Stress and the Integrative Behaviour and Neuroscience Group at UTSC.

LITERATURE CITED

- Atwood HL, Govind CK, Wu CF. 1993. Differential ultrastructure of synaptic terminals on ventral longitudinal abdominal muscles in *Drosophila* larvae. *J Neurobiol* 24:1008–1024.
- Babcock M, Macleod GT, Leither J, Pallanck L. 2004. Genetic analysis of soluble N-ethylmaleimide-sensitive factor attachment protein function in *Drosophila* reveals positive and negative secretory roles. *J Neurosci* 24:3964–3973.
- Block MR, Glick BS, Wilcox CA, Wieland FT, Rothman JE. 1988. Purification of an N-ethylmaleimide-sensitive protein catalyzing vesicular transport. *Proc Natl Acad Sci U S A* 85:7852–7856.
- Boulianne GL, Trimble WS. 1995. Identification of a second homolog of N-ethylmaleimide-sensitive fusion protein that is expressed in the nervous system and secretory tissues of *Drosophila*. *Proc Natl Acad Sci U S A* 92:7095–7099.
- Broadie KS, Bate M. 1993. Development of the embryonic neuromuscular synapse of *Drosophila melanogaster*. *J Neurosci* 13:144–166.
- Clary DO, Griff IC, Rothman JE. 1990. SNAPs, a family of NSF attachment proteins involved in intracellular membrane fusion in animals and yeast. *Cell* 61:709–721.
- Cole JC, Villa BR, Wilkinson RS. 2000. Disruption of actin impedes transmitter release in snake motor terminals. *J Physiol* 525(Pt 3):579–586.
- Cong M, Perry SJ, Hu LA, Hanson PI, Claing A, Lefkowitz RJ. 2001. Binding of the beta2 adrenergic receptor to N-ethylmaleimide-sensitive factor regulates receptor recycling. *J Biol Chem* 276:45145–45152.
- Cooper RL, Marin L, Atwood HL. 1995. Synaptic differentiation of a single motor neuron: conjoint definition of transmitter release, presynaptic calcium signals, and ultrastructure. *J Neurosci* 15:4209–4222.
- Cooper RL, Winslow JL, Govind CK, Atwood HL. 1996. Synaptic structural complexity as a factor enhancing probability of calcium-mediated transmitter release. *J Neurophysiol* 75:2451–2466.
- Coyle IP, Koh YH, Lee WC, Slind J, Fergestad T, Littleton JT, Ganetzky B. 2004. Nervous wreck, an SH3 adaptor protein that interacts with Wsp, regulates synaptic growth in *Drosophila*. *Neuron* 41:521–534.
- Deitcher DL, Ueda A, Stewart BA, Burgess RW, Kidokoro Y, Schwarz TL. 1998. Distinct requirements for evoked and spontaneous release of neurotransmitter are revealed by mutations in the *Drosophila* gene neuronal-synaptobrevin. *J Neurosci* 18:2028–2039.
- DiAntonio A, Schwarz TL. 1994. The effect on synaptic physiology of synaptotagmin mutations in *Drosophila*. *Neuron* 12:909–920.
- Doussau F, Augustine GJ. 2000. The actin cytoskeleton and neurotransmitter release: an overview. *Biochimie* 82:353–363.
- Golby JA, Tolar LA, Pallanck L. 2001. Partitioning of N-ethylmaleimide-sensitive fusion (NSF) protein function in *Drosophila melanogaster*: dNSF1 is required in the nervous system, and dNSF2 is required in mesoderm. *Genetics* 158:265–278.
- Han SY, Park DY, Park SD, Hong SH. 2000. Identification of Rab6 as an N-ethylmaleimide-sensitive fusion protein-binding protein. *Biochem J* 352(Pt 1):165–173.
- Hepp R, Langley K. 2001. SNAREs during development. *Cell Tissue Res* 305:247–253.
- Kimura K, Mizoguchi A, Ide C. 2003. Regulation of growth cone extension by SNARE proteins. *J Histochem Cytochem* 51:429–433.
- Lavolette MJ, Nunes P, Peyre J-B, Aigaki T, Stewart BA. 2005. A genetic screen for suppressors of *Drosophila* NSF2 neuromuscular junction overgrowth. *Genetics* DOI 10.1534/genetics.104.035691 [Epub ahead of print].
- Llinas R, Sugimori M, Silver RB. 1992. Microdomains of high calcium concentration in a presynaptic terminal. *Science* 256:677–679.
- Martinez-Arca S, Alberts P, Zahraoui A, Louvard D, Galli T. 2000. Role of tetanus neurotoxin insensitive vesicle-associated membrane protein (TI-VAMP) in vesicular transport mediating neurite outgrowth. *J Cell Biol* 149:889–900.
- Mohtashami M, Stewart BA, Boulianne GL, Trimble WS. 2001. Analysis of the mutant *Drosophila* N-ethylmaleimide sensitive fusion-1 protein in comatose reveals molecular correlates of the behavioural paralysis. *J Neurochem* 77:1407–1417.
- Morales M, Colicos MA, Goda Y. 2000. Actin-dependent regulation of neurotransmitter release at central synapses. *Neuron* 27:539–550.
- Morgan A, Burgoyne RD. 1995. A role for soluble NSF attachment proteins (SNAPs) in regulated exocytosis in adrenal chromaffin cells. *EMBO J* 14:232–239.
- Nishimune A, Isaac JT, Molnar E, Noel J, Nash SR, Tagaya M, Collingridge GL, Nakanishi S, Henley JM. 1998. NSF binding to GluR2 regulates synaptic transmission. *Neuron* 21:87–97.
- Noel J, Ralph GS, Pickard L, Williams J, Molnar E, Uney JB, Collingridge GL, Henley JM. 1999. Surface expression of AMPA receptors in hippocampal neurons is regulated by an NSF-dependent mechanism. *Neuron* 23:365–376.
- Osen-Sand A, Catsicas M, Staple JK, Jones KA, Ayala G, Knowles J, Grenningloh G, Catsicas S. 1993. Inhibition of axonal growth by SNAP-25 antisense oligonucleotides in vitro and in vivo. *Nature* 364:445–448.
- Osten P, Srivastava S, Inman GJ, Vilim FS, Khatri L, Lee LM, States BA, Einheber S, Milner TA, Hanson PI, Ziff EB. 1998. The AMPA receptor GluR2 C terminus can mediate a reversible, ATP-dependent interaction with NSF and alpha- and beta-SNAPs. *Neuron* 21:99–110.
- Pallanck L, Ordway RW, Ramaswami M, Chi WY, Krishnan KS, Ganetzky B. 1995. Distinct roles for N-ethylmaleimide-sensitive fusion protein (NSF) suggested by the identification of a second *Drosophila* NSF homolog. *J Biol Chem* 270:18742–18744.
- Phillips GR, Huang JK, Wang Y, Tanaka H, Shapiro L, Zhang W, Shan WS, Arndt K, Frank M, Gordon RE, Gawinowicz MA, Zhao Y, Colman DR. 2001. The presynaptic particle web. Ultrastructure, composition, dissolution, and reconstitution. *Neuron* 32:63–77.
- Sagiv Y, Legesse-Miller A, Porat A, Elazar Z. 2000. GATE-16, a membrane transport modulator, interacts with NSF and the Golgi v-SNARE GOS-28. *EMBO J* 19:1494–1504.
- Sakaba T, Neher E. 2003. Involvement of actin polymerization in vesicle recruitment at the calyx of Held synapse. *J Neurosci* 23:837–846.
- Sankaranarayanan S, Atluri PP, Ryan TA. 2003. Actin has a molecular scaffolding, not propulsive, role in presynaptic function. *Nat Neurosci* 6:127–135.
- Schulze KL, Broadie K, Perin MS, Bellen HJ. 1995. Genetic and electro-

- physiological studies of *Drosophila* syntaxin-1A demonstrate its role in nonneuronal secretion and neurotransmission. *Cell* 80:311–320.
- Shupliakov O, Bloom O, Gustafsson JS, Kjaerulff O, Low P, Tomilin N, Pieribone VA, Greengard P, Brodin L. 2002. Impaired recycling of synaptic vesicles after acute perturbation of the presynaptic actin cytoskeleton. *Proc Natl Acad Sci U S A* 99:14476–14481.
- Sollner T, Whiteheart SW, Brunner M, Erdjument-Bromage H, Geromanos S, Tempst P, Rothman JE. 1993. SNAP receptors implicated in vesicle targeting and fusion. *Nature* 362:318–324.
- Song I, Kamboj S, Xia J, Dong H, Liao D, Hagan RL. 1998. Interaction of the N-ethylmaleimide-sensitive factor with AMPA receptors. *Neuron* 21:393–400.
- Stewart BA, Atwood HL, Renger JJ, Wang J, Wu CF. 1994. Improved stability of *Drosophila* larval neuromuscular preparations in haemolymph-like physiological solutions. *J Comp Physiol [A]* 175:179–191.
- Stewart BA, Schuster CM, Goodman CS, Atwood HL. 1996. Homeostasis of synaptic transmission in *Drosophila* with genetically altered nerve terminal morphology. *J Neurosci* 16:3877–3886.
- Stewart BA, Mohtashami M, Trimble WS, Boulianne GL. 2000. SNARE proteins contribute to calcium cooperativity of synaptic transmission. *Proc Natl Acad Sci U S A* 97:13955–13960.
- Stewart BA, Mohtashami M, Zhou L, Trimble WS, Boulianne GL. 2001. SNARE-dependent signaling at the *Drosophila* wing margin. *Dev Biol* 234:13–23.
- Stewart BA, Mohtashami M, Rivlin P, Deitcher DL, Trimble WS, Boulianne GL. 2002. Dominant-negative NSF2 disrupts the structure and function of *Drosophila* neuromuscular synapses. *J Neurobiol* 51:261–271.
- Vilinsky I, Stewart BA, Drummond J, Robinson I, Deitcher DL. 2002. A *Drosophila* SNAP-25 null mutant reveals context-dependent redundancy with SNAP-24 in neurotransmission. *Genetics* 162:259–271.
- Whiteheart SW, Matveeva EA. 2004. Multiple binding proteins suggest diverse functions for the N-ethylmaleimide sensitive factor. *J Struct Biol* 146:32–43.
- Whiteheart SW, Rossmagel K, Buhrow SA, Brunner M, Jaenicke R, Rothman JE. 1994. N-ethylmaleimide-sensitive fusion protein: a trimeric ATPase whose hydrolysis of ATP is required for membrane fusion. *J Cell Biol* 126:945–954.
- Xu Z, Sato K, Wickner W. 1998. LMA1 binds to vacuoles at Sec18p (NSF), transfers upon ATP hydrolysis to a t-SNARE (Vam3p) complex, and is released during fusion. *Cell* 93:1125–1134.
- Yu FR, Guan Z, Zhuo M, Sun LY, Zou WG, Zheng ZC, Liu XY. 2002. Further identification of NSF* as an epilepsy related gene. *Mol Brain Res* 99:141–144.
- Zhang W, Benson DL. 2001. Stages of synapse development defined by dependence on F-actin. *J Neurosci* 21:5169–5181.